

RESEARCH PAPER

## Targeted detection of the cancer cells using the anti-CD24 bio modified PEGylated gold nanoparticles: the application of CD24 as a vital cancer biomarker

Mona Fazel-Ghaziyani<sup>1</sup>, Daryoush Shahbazi-Gahrouei<sup>1\*</sup>, Mohammad Pourhassan-Moghaddam<sup>2,3</sup>, Behzad Baradaran<sup>3</sup>, Mostafa Ghavami<sup>4</sup>

<sup>1</sup>Department of Medical Physics, School of Medicine, Isfahan University of Medical Sciences, Isfahan, Iran

<sup>2</sup>Department of Medical Biotechnology, Faculty of Advanced Medical Sciences, Tabriz University of Medical Sciences, Tabriz, Iran

<sup>3</sup>Immunology Research Center, Tabriz University of Medical Sciences, Tabriz, Iran

<sup>4</sup>Department of Radiology, Paramedical School, Tabriz University of Medical Sciences, Tabriz, Iran

### ABSTRACT

**Objective(s):** The central role of molecular imaging modalities in cancer management is an undeniable fact that could help to diagnose cancer tumors in early stages. The main aim of this study is to prepare a novel targeted molecular imaging nanoprobe of CD24-PEGylated Au NPs to improve the ability of Computed tomography scanning (CT scan) outputs for both in vitro and in vivo detection of breast cancer (4T1) cells.

**Materials and Methods:** Gold nanoparticles (Au NPs) were synthesized and coated with polyethylene glycol (PEG) chains in order to improve the stability of the Au NPs and to provide bio modification points for antibody immobilization. The synthesized nanoprobe was used for both in vitro and in vivo targeted CT imaging breast cancer cells (4T1) and the xenograft tumor model.

**Results:** Findings showed that the attenuation coefficient of 4T1 cells that were targeted by CD24-PEGylated Au NPs is calculated to be over two times higher than the untargeted 4T1 cells (15 HU vs 39 HU, respectively). Indeed, the results clearly reveal that the developed CD24-PEGylated Au NPs showed the tumor CT enhancement was higher than that of Omnipaque which used as control.

Also, the CT number values of the tumor area at different time points gradually increased after 60 min post injection and was significantly higher than before injection.

**Conclusions:** Results showed the introduced CT imaging nanoprobe (Au NPs-PEGylated) could be useful for CT imaging of breast tumors under in vivo condition. Overall, it is concluded that Au NPs-PEGylated contrast media is able to detect breast cancer (4T1) cells and is more effective compared with other casual methods.

**Keyword:** CD24 antibody, Computed tomography, Cancer detection, Gold nanoparticle, Polyethylene glycol (PEG), 4T1

### How to cite this article

Fazel-Ghaziyani M, Shahbazi-Gahrouei D, Pourhassan-Moghaddam M, Baradaran B, Ghavami M. Targeted detection of the cancer cells using the anti-CD24 bio modified PEGylated gold nanoparticles: the application of CD24 as a vital cancer biomarker. *Nanomed J.* 2018; 5(3): 172-179. DOI: 10.22038/nmj.2018.005.0007

### INTRODUCTION

Currently, imaging modalities have been considered for detection and recognition treatment progress in various diseases, especially cancer. Cancer imaging could be divided into two categories: (i) structural (anatomical) imaging and (ii) molecular imaging (functional) [1] modalities.

Computed Tomography (CT), Magnetic Resonance Imaging (MRI), and Ultrasound methods as the (anatomical) structural imaging applications are applying in clinical domain in order to detect different cancer progress steps such as propagation and tumor site. Also, anatomical information could be obtained through the mentioned structural imaging applications for treatment aims [2]. Despite much valuable information from the structural imaging modalities, there are some dramatic limitations concerning cancer detection,

\* Corresponding Author Email: [shahbazi@med.mui.ac.ir](mailto:shahbazi@med.mui.ac.ir)

Note. This manuscript was submitted on May 15, 2018; approved on June 21, 2018

including lack of distinction between benign and malignant tumors and inability to recognize of metastases less than 0.5 cm [3, 4]. Molecular imaging based on incorporation molecular biology and in vivo imaging techniques has been implemented recently to gain more data on biological condition of diseases through molecular markers. To achieve molecular imaging outputs, it is necessary to obtain anatomical imaging system using targeted contrast media [5-7]. CT is a potent diagnostic imaging device that is low expensive, deep tissue permeation, great spatial, and density resolution [8, 9]. Clinically, molecular composition of iodine is mostly exerted as a contrast operator in CT imaging [10]. It is include some drawbacks such as possibility of renal toxicity, insufficient circulation time for long time imaging, and deficiency of targeting specificity. These defects are the main problems for misleading results concerning biological ingredient or cancer markers [9, 11, 12]. Therefore, in spite of some appropriate properties of the contrast operator, it is not a suitable molecular imaging modality for sensitive and selective operations. Since high sensitivity and selectivity are two crucial factors in cancer detection, designing novel nanoprobe with the mentioned characterizations have been considered in the recent years [13].

To achieve these aims, nanoparticles (NPs) have been notified for preparing high-performance contrast media for CT method. Nanoparticles contain various appropriate properties for this purpose, including high number of atoms (radio-dense elements), flexible surface characteristics for attaching biomarker, suitable shape and size for cell entrance automatically, ability to be functionalized for targeting goals such as monoclonal antibodies, and selectivity cellular uptake [14-17]. Gold nanoparticles (Au NPs) due to the eligible colloid endurance, well bio-adaptability, easy synthesis, controlling their sizes, and surface modification flexibility are widely used in the many biological researches [18-20]. Moreover, since Au NPs include tunable surface, they could easily be conjugated with targeting ligands such as antibodies [21-24]. However, Au NPs are unstable under physiological conditions and they easily could aggregate [11, 25]. To overcome these problems, since polyethylene glycol (PEG) prevents plasma proteins interactions with the NPs, the surface of Au NPs is often modified with PEG chains to increase the dispensability and

blood retention [26, 27]. Therefore, through the mentioned method targeted CT imaging of tumors could be achieved with high reliability.

From the many researches, CD24 as a surface marker is expressed in the high level in a wide range of solid tumors such as carcinoma of renal cell, nasopharyngeal, hepatocellular, bladder, breast cancer, ovarian cancer and lung cancer [28-32]. It is shown that CD24 has a direct connection with the metastasis capacity of the solid tumors through interaction with P-selection as an adhesion receptor on activated endothelial cells and platelets [33]. Many studies revealed that CD24 as biomarker could be helpful in the clinical domain to choose a suitable treatment [34]. Furthermore, according to the specific properties of CD24, it is a well biomarker for conjugation to NPs. The main aim of this study is to use a targeted PEGylated gold nanoparticle with CD24 antibody for both in vitro and in vivo detection of cancer cells (4T1).

## MATERIALS AND METHODS

### Materials

### Chemical synthesis, Bio conjugation and Characterization of Au NP

Chemical synthesis was carried out by the citrate reduction method as introduced elsewhere (R). The synthesized Au NPs were PEGylated with a mixture of long PEG (HS-PEG-CH<sub>3</sub>O; MW = 6000) and short PEG (HS-PEG-COOH; MW = 3500) using a molar ratio of 1 to 3 in water for 72 hours. The terminal carboxylate groups were then activated with 3  $\mu$ L of (1-ethyl-3-(3-dimethylaminopropyl) carbodiimide hydrochloride) EDC (0.4 M) and (N-hydroxysuccinimide) NHS (0.1 M) for 10 min. After centrifugation at 5000 rpm for 5 min, the supernatant was removed and the pellet was redispersed with 80  $\mu$ L of PBS buffer. Afterward, 20  $\mu$ L of the antibody (0.5 mg/mL) was added into the tube and incubated for 2 hr at RT. The morphology of the provided Au NPs was characterized via transmission electron microscopy (TEM) imaging (2010F JEOL analytical electron microscope, Japan) with an operating voltage of 100 kV. An aqueous solution of a sample (5 mL, 1 mg/mL) was dropped onto a carbon-coated copper grid and air dried before measurements.

### Cell culture

4T1 (mouse breast cancer) and CT26 (mouse colorectal cancer) cell lines were purchased from

Pasteur institute, Tehran, Iran. The cells were continuously cultured in the supplemented RPMI 1640 medium with (fetal bovine serum) FBS (10%) and penicillin/streptomycin (1%). The cultured cells were incubated at 37 °C and 5% CO<sub>2</sub> in a humidified atmosphere.

#### **Evaluation of the biocompatibility using MTT assay**

The biocompatibility of CD24-PEGylated Au NPs was studied through a tetrazolium dye MTT assay. Briefly, the cells in early log phase were trypsinized and cultured in 96-well plates with concentration of 10<sup>4</sup> cells/well/200 µl. Then, they were incubated overnight at 37 °C and 5% CO<sub>2</sub>. After 24 h, the stock medium was replaced with the fresh medium, containing different concentrations of CD24-PEG-Au NPs (0, 0.005, 0.01, 0.02, 0.05 and 0.1 mM). After 4 hr of treatments, 50 µl MTT (2 mg/ml) was added to each well and incubated for 4 h in a humidified atmosphere at 37 °C following the manufacturer's instructions. The formazan crystals were solubilized with DMSO (dimethyl sulfoxide) and 25 µl of Sorenson buffer. Then, the absorbance at a wavelength of 570 nm was measured using ELISA plate reader (Bio Teck, Germany). All experiments were performed at least three times. To analyze obtained data, the peak of absorbance was considered for each concentration and the viability percentage was calculated based on the following formula: Percentage cell viability (%) = (mean absorbance of test/mean absorbance of control) × 100.

#### **CT number measurement**

Ten consecutive dilutions of PEGylated Au NPs or iohexol as a common contrast media (Omnipaque®, 300 mg iodine per ml, GE Healthcare, Milwaukee, WI, USA) were provided by in 1.5 ml micro tube through using different concentrations of [Au] or [I] (from 0.005 to 1 mM). Then, the obtained solutions were placed in a self-designed scanning holder. Distilled water sample was used to normalize X-ray absorption. The provided tubes were then scanned using a 16 row multi detector CT system (Bright Speed VCT, GE Medical Systems, Milwaukee, WI, USA) with the following sets: tube voltage: 120 kV; tube current: 150 mA; slice thickness: 0.625 mm; slice space: 0, and CT number measured using a GE imaging workstation (Advantage Workstation 4.3, GE Medical Systems, Milwaukee, WI, USA). A 5

mm circle as region of interest (ROI) was laid over the center of each image in five different slices to measure CT value. The data were presented as mean ± standard deviation.

#### **In vitro CT imaging of cancer cells**

4T1 cells were cultured in a 6-well plate at a density of 1.5 × 10<sup>6</sup> cells/well one day prior to the experiment. The cells culture medium was replaced with fresh medium containing CD24-PEGylated-Au NPs at 0.1 mM concentrations and the cells were incubated for 3 h at 37 °C and 5% CO<sub>2</sub>. CT26 cell line in the presence CD24-PEGylated-AuNPs, and 4T1 cell line in the presence IgG-PEGylated-Au NPs were used as control samples in the same concentrations. The cells were washed with PBS three times for 5 min, then, trypsinized. Following that, the washed cells were centrifuged, and resuspended in 200 µl PBS in 0.5 ml Eppendorf tubes. Also, 200 µl water in 0.5 ml Eppendorf tube was used as a control sample for normalizing absorption. The supplied tubes were placed in a self-designed scanning holder. Finally, the cells suspension samples were scanned by using mentioned CT imaging system.

#### **Targeted Computed Tomography imaging of 4T1 tumor in vivo**

All animal experiments and cares were performed according to the protocols approved by the institutional committee for animal care and the policy of the National Ministry. In the initial stage, female 4-6-week-old BALB/C mice (18-20 g, Pasteur Institute, Tehran, Iran) were subcutaneously injected with 1 × 10<sup>6</sup> cells/mouse in the abdominal mammary gland. Following this, the tumor nodules were allowed to reach their volumes of 0.7-1.2 cm<sup>3</sup> after approximately 2 weeks post injection. Then, after the mice were anesthetized by intraperitoneal injection 0.2 ml of Xylazine 2% and Ketamine hydrochloric, they were placed in a scanning holder and injected with CD24-PEGylated Au NPs and Omnipaque (100 mL, [Au] 1 mM). Finally, the injected mice were scanned immediately as a first time point 0 and in the delay times of 30 and 60 min post injection and next prepared images were reconstructed on CT imaging workstation (Advantage Workstation 4.3, GE Medical Systems, Milwaukee, WI, USA). Meanwhile, CT scanning was performed before injection as a control images and it is noticeable that the same CT imaging system and protocol were used for in vitro and in vivo imaging.

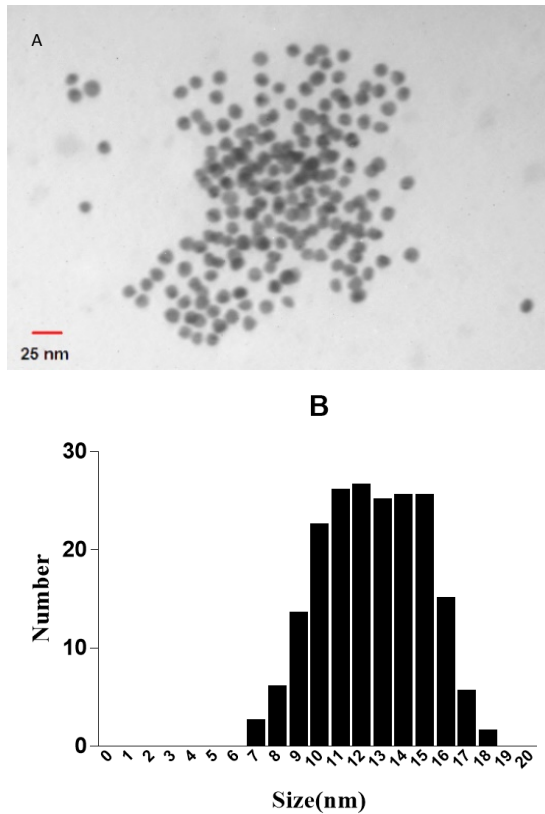


Fig 1. (A) TEM image of gold nanoparticles and (B) histogram of size distribution. The gold nanoparticles were observed to be 10-15 nm in diameter and as quasi-spherical shapes on the TEM image

## RESULT AND DISCUSSION

### Synthesis and Characterization of CD24 modified Au NPs

To prepare desired nanoparticles as a CT targeted contrast media, gold nanoparticles were covered via PEG/ m-PEG chains effectively in order to improve biocompatibility and decrease aggregation of the NPs [34-36]. As mentioned in researches the addition of PEG to NPs increases circulation time that is so important for imaging applications [37, 38]. In addition to use of the PEG, changes NP size for this reason the EPR effect was modulated and solubility in buffer and serum increases due to the hydrophilic ethylene glycol repeats [39]. The coated NPs with PEG and m-PEG are able to be conjugated with the antibody easily [29]. The terminal end of PEG can be activated by EDC/NHS groups and it attached to CD24; it would give some unique characteristics to the NPs such as appropriate size, biocompatibility, and maximum wave length that to be implemented in the in vitro and in vivo experiments. As it is shown in figure

1A, the archived Au NPs include a spherical shape in the TEM image. Also, the prepared Au NPs were a red-colored solution with a particles size range from 10 to 15 nm in diameter (Fig 1B).

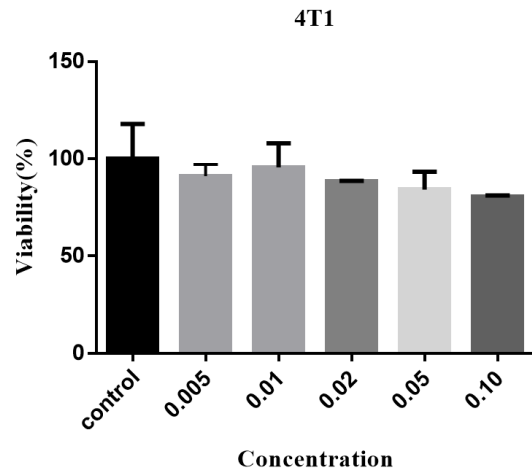


Fig 2. Viability of 4T1 cells after treatment with CD24-PEGylated-Au NPs at the different Au concentrations for 4 hr

### Cytotoxicity assay

Before application of the formed CD24-PEGylated-Au NPs as a contrast media for in vitro CT imaging, the cytotoxicity effects of the modified NPs were analyzed via MTT viability assays. In order to examine the viability of 4T1 cells, the cell line was treated in the presence CD24-PEGylated-Au NPs for 4 h. As it is shown in Fig 2, there were no significant changes in the different concentrations of Au compared with the treated control cell line with PBS buffer ( $P > 0.05$ ). From the obtained results, it is suggested that the modified NPs are compatible in the different concentrations of Au under biological condition.

### X-ray attenuation property of NPs

Since gold atom contains higher atomic number and electron density compared to iodine, it is expected that this atom would show a greater X-ray absorption coefficient [36]. Some studies proved this theory and showed the attenuation coefficient difference in concentration greater than 0.01 M [35]. In this study X-ray attenuation of prepared PEGylated Au nanoparticles was compared with that of Omnipaque in ten serial dilutions whereas water absorption used as normalized all the absorption data. The concentrations of Au and iodine were less than 1 mM in all samples. It was revealed that with the increment concentrations of the radio dense

elements (Au and I), X-ray attenuation coefficients for both PEGylated Au NPs and Omnipaque were risen (Fig 3b), but difference in CT number is low as observed in CT images (Fig 3a) and quantitative study was used to show that difference. While, in the presence PEGylated Au NPs, the risen rate of X-ray attenuation was slightly higher than that of iohexol. Despite using slight differences in the concentrations Au and iodine (lower than 1 mM), according to the capability of PEGylated Au NPs to conjugate with CD24 antibody, this minor difference in the radiation absorption was used for computed tomography.

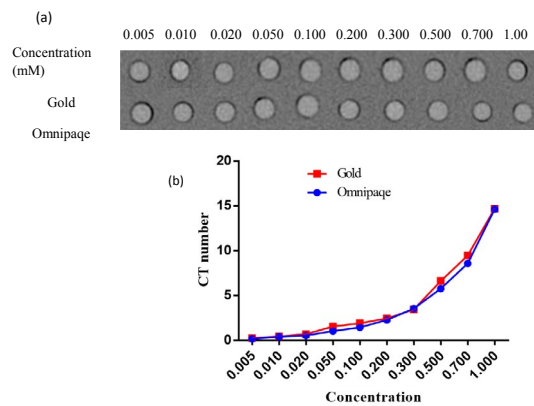


Fig 3. CT images (a) and X-ray attenuation (HU) intensity (b) of PEGylated Au NPs and omnipaque as a function of the mM concentration of radio dense element (Au and iodine)

**In vitro CT imaging of cancer cells**

To carry out CT imaging experiment,  $10^6$  cells/mL (4T1 cells) was used. As previously discussed, 4T1 cells has a significant CD24 overexpression. CT imaging was performed on the cells that were targeted by anti CD24 coated PEGylating gold nanoparticles (CD24-PEGylated Au NPs). In this experiment there were three negative control including; CT imaging of 4T1 cells (breast cancer) in the absence of the NPs, CT imaging of 4T1 cells that were targeted by IgG- PEGylated Au NPs (unspecific antibody), and CT imaging of CT26 cells (colorectal cancer) that does not express this antigen, in the presence of CD24-PEGylated Au NPs. Since it is difficult to investigate the brightness difference of the cell in CT images (Fig 4a), quantitative analysis of the CT values of the images was necessary. Figure 4b shows the attenuation values in Hounsfield unit (HU) that were obtained from CT imaging experiments. The attenuation coefficient of 4T1 cells that were

targeted by CD24-PEGylated Au NPs is calculated to be over two times higher than the untargeted 4T1 cells (15 HU vs 39 HU, respectively). The achieved values obviously illustrated that the targeted NPs were attached to 4T1 cells. The attenuation values of the negative control samples indicated that nonspecific binding was comparatively rare in the samples. Surrounding 4T1 cells through CD24-PEGylated Au NPs is responsible for increasing the rate of radiation absorption by the cells. Since 0.1 mM of CD24-PEGylated Au NPs was used in this section, from the previous researches, it includes less complication compared with other contrast media [27, 36].

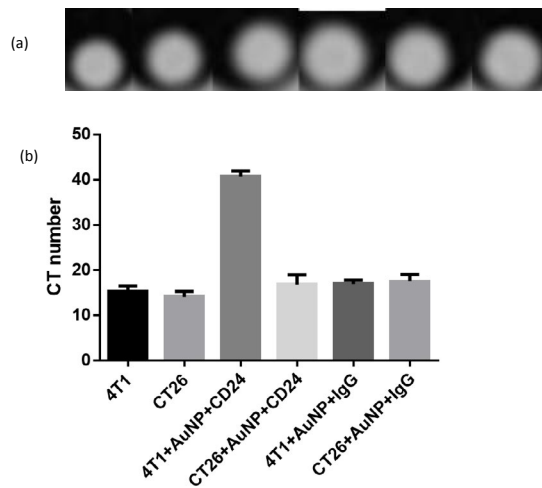


Fig 4. CT images (a) and x-ray attenuation intensity (b) of 4T1 and CT26 cell lines after incubation with nanoparticles

**Targeted CT imaging of 4T1 cells in vivo**

With the suitable biocompatibility and targeting specificity of CD24-PEGylated Au NPs, the applicability of CD24-PEGylated Au NPs for in vivo targeted CT imaging of 4T1 cells was investigated. Whereas early detection of cancer is a fundamental factor for planning effective therapeutic intervention; therefore, for this reason a small xenografted 4T1 tumor model was established in BALB/C mice and subsequently, the CT number of the tumor region was quantified before injection and after different time points post injection. According to the CT images of tumor before and after intravenous injection of CD24-PEGylated Au NPs (Fig 5a), it's quiet clear that the tumor site showed an enhancement of higher CT value after injection compared with that in control. Quantitative CT help us to clarify the amount of this enhancement. Overall, it's evident

that the CT values of the tumor area at different time points gradually increased (Fig 6); after 60 min post injection, the CT value was significantly higher than before injection ( $P < 0.05$  Fig 6). These results clearly reveal that in addition to the developed CD24-PEGylated Au NPs could be useful for CT imaging of breast tumors in vivo, the tumor CT enhancement is higher than that of Omnipaque (Fig 5 and Fig 6).

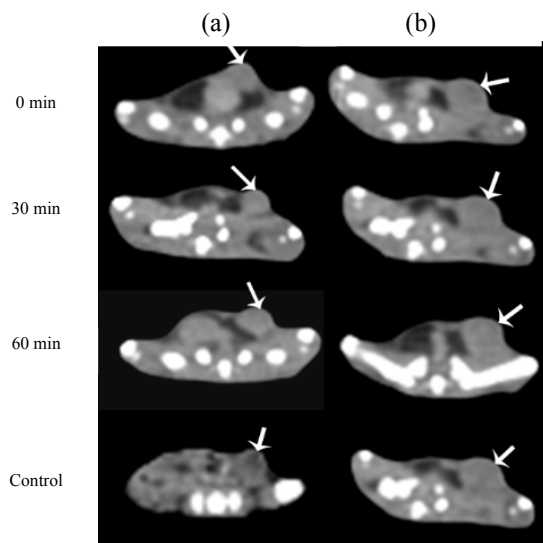


Fig 5. CT image of mice bearing 4T1 tumor after intravenous injection of the prepared nanoparticles (a) control mice were injected with Omnipaque (b). Images were taken before 0, 30 and 60 min post injection. Tumor region was showed with white arrow

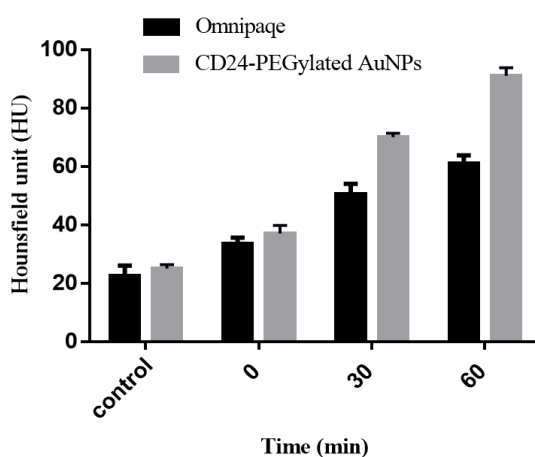


Fig 6. CT value in Hounsfield unit (HU) of the tumor region before injection and at different time points post injection

## CONCLUSION

Using cancer biomarker in CT imaging has been developed reliably as an inexpensive way for classification tumors. CD24 antibody as biomarker for detection and characterization of cell cancer was conjugated to the Au NPs PEGylated and used as a targeted contrast mediate for the detection of breast cancer 4T1 cells both in vitro and in vivo. The obtained results illustrated that the introduced nanoprobe is able to help detecting the existence of cancer cells that express CD24 through clinical CT scans. With the provided this new nanoprobe, it is expected that this method would be useful for cancer detection in different stages.

## ACKNOWLEDGMENTS

This work is a part of PhD thesis which financially (Grant No. 395550) supported by Isfahan University of Medical Sciences, Isfahan, Iran.

## CONFLICTS OF INTEREST

The authors declare that they have no conflict of interest.

## REFERENCES

- Bernstein AI, Dhanantwari A, Jurcova M, Cheheltani R, Naha PC, Ivanc T, Shefer E, Cormode DP, Improved sensitivity of computed tomography towards iodine and gold nanoparticle contrast agents via iterative reconstruction methods. *Sci Rep.* 2016; 17: 6: 26177.
- Nanni C, Rubello D, Fanti S, Farsad M, Ambrosini V, Rampin L, Banti E, Carpi A, Muzzio P, Franchi R, Role of 18F-FDG-PET and PET/CT imaging in thyroid cancer. *Biomed Pharmacoth.* 2006; 60(8): 409-413.
- Herschman HR, Molecular imaging: looking at problems, seeing solutions. *Science.* 2003; 302(5645), 605-608.
- Hussain T, Nguyen QT, Molecular imaging for cancer diagnosis and surgery. *Adv Drug Deliv Rev.* 2014; 66, 90-100.
- Moradi Khaniabadi PD, Shahbazi-Gahrouei M, Suhaimi Jaafar MAA, Majid Shah B, Moradi Khaniabadi S, Shahbazi-Gahrouei. Magnetic iron oxide nanoparticles as T2 MR imaging contrast agent for detection of breast cancer (MCF-7) cell. *Avicenna J Med Biotechnol.* 2017; 9(4): 181-188.
- James ML, Gambhir SS, A molecular imaging primer: modalities, imaging agents, and applications. *Physiol Rev.* 2012; 92(2): 897-965.
- Kircher MF, Willmann JK, Molecular body imaging: MR imaging, CT, and US. Part I. Principles. *Radiology.* 2012; 263(3): 633-643.
- Hyafil F, Cornily JC, Feig JE, Gordon R, Vucic E, Amirbekian V, Fisher EA, Fuster V, Feldman LJ, Fayad ZA, Noninvasive detection of macrophages using a nanoparticulate contrast agent for computed tomography. *Nat Med.* 2007; 13(5): 636-641.

9. Liu H, Xu Y, Wen S, Chen Q, Zheng L, Shen M, Zhao J, Zhang G, Shi X, Targeted tumor computed tomography imaging using low-generation dendrimer-stabilized gold nanoparticles. *Chem-Eur J*. 2013; 19 (20): 6409-6416.
10. Sharifian S, Shahbazi-Gahrouei D. Dose Assessment in multidetector computed tomography (CT) of polymethylmethacrylate (PMMA) phantom using American Association of Physicists in Medicine-Task Group Report No. 111 (AAPM-TG111). *J Isfahan Med Sch*. 2017; 35(421): 200-205.
11. Wang H, Zheng L, Peng C, Shen M, Shi X, Zhang G, Folic acid-modified dendrimer-entrapped gold nanoparticles as nanoprobes for targeted CT imaging of human lung adenocarcinoma. *Biomaterials*. 2013; 34 (2): 470-480.
12. Keshtkar M, Shahbazi-Gahrouei D, Khoshfetrat SM, Mehrgardi MA, Aghaei M. Aptamer-conjugated magnetic nanoparticles as targeted magnetic resonance imaging contrast agent for breast cancer. *J Med Sign Sens*. 2016; 6(4): 243-247.
13. Li Y, Qi X, Lei C, Yue Q, Zhang S. Simultaneous SERS detection and imaging of two biomarkers on the cancer cell surface by self-assembly of branched DNA-gold nanoaggregates. *Chem Commun (Camb)*2014; 50(69): 9907-9909.
14. Ai K, Liu Y, Liu J, Yuan Q, He Y, Lu L, Large-scale synthesis of Bi(2)S(3) nanodots as a contrast agent for in vivo X-ray computed tomography imaging. *Adv Mater*. 2011; 23(42): 4886-4891.
15. Gratton SE, Ropp PA, Pohlhaus PD, Luft JC, Madden VJ, Napier ME, DeSimone JM. The effect of particle design on cellular internalization pathways. *Roc Natl Acad Sci U S A*. 2008; 105(33): 11613-11618.
16. Huang X, Teng X, Chen D, Tang F, He J. The effect of the shape of mesoporous silica nanoparticles on cellular uptake and cell function. *Biomaterials*. 2010; 31(3): 438-448.
17. Ghahremani F, Shahbazi-Gahrouei D, Kefayat A, Motaghi H, Mehrgardi MA, Javanmard SH. AS1411 aptamer conjugated gold nanoclusters as a targeted radiosensitizer for megavoltage radiation therapy of 4T1 breast cancer cells. *RSC Adv*. 2018; 8: 4249-4258.
18. Lesniak A, Fenaroli F, Monopoli MP, Aberg C, Dawson KA, Salvati A. Effects of the presence or absence of a protein corona on silica nanoparticle uptake and impact on cells. *ACS nano*. 2012; 6(7): 5845-5857.
19. Shang L, Nienhaus K, Nienhaus GU. Engineered nanoparticles interacting with cells: size matters. *J Nanobiotechnology*. 2014; 12, 5.
20. Wolfram J, Yang Y, Shen J, Moten A, Chen C, Shen H, Ferrari M, Zhao Y. The nano-plasma interface: Implications of the protein corona. *Colloids Surf B Biointerfaces*. 2014; 124: 17-24.
21. Peng C, Li K, Cao X, Xiao T, Hou W, Zheng L, Guo R, Shen M, Zhang G, Shi X. Facile formation of dendrimer-stabilized gold nanoparticles modified with diatrizoic acid for enhanced computed tomography imaging applications. *Nanoscale*. 2012; 4(21): 6768-78.
22. Peng C, Zheng L, Chen Q, Shen M, Guo R, Wang H, Cao X, Zhang G, Shi X. PEGylated dendrimer-entrapped gold nanoparticles for in vivo blood pool and tumor imaging by computed tomography. *Biomaterials*. 2012; 33(4): 1107-1119.
23. Reuveni T, Motiei M, Romman Z, Popovtzer A, Popovtzer R, Targeted gold nanoparticles enable molecular CT imaging of cancer: an in vivo study. *Int J Nanomedicine*. 2011; 6: 2859-2864.
24. Wang H, Zheng L, Peng C, Guo R, Shen M, Shi X, Zhang G. Computed tomography imaging of cancer cells using acetylated dendrimer-entrapped gold nanoparticles. *Biomaterials*. 2011; 32(11): 2979-2988.
25. Acharya S, Sahoo SK. PLGA nanoparticles containing various anticancer agents and tumour delivery by EPR effect. *Adv Drug Deliv Rev*. 2011; 63(3): 170-183.
26. Aggarwal P, Hall JB, McLeland CB, Dobrovolskaia MA, McNeil SE. Nanoparticle interaction with plasma proteins as it relates to particle biodistribution, biocompatibility and therapeutic efficacy. *Adv Drug Deliv Rev*. 2009; 61(6): 428-437.
27. Nakagawa T, Gonda K, Kamei T, Cong L, Hamada Y, Kitamura N, Tada H, Ishida T, Aimiya T, Furusawa N, Nakano Y, Ohuchi N. X-ray computed tomography imaging of a tumor with high sensitivity using gold nanoparticles conjugated to a cancer-specific antibody via polyethylene glycol chains on their surface. *Sci Technol Adv Mater*. 2016; 17(1): 387-397.
28. Droz D, Zachar D, Charbit L, Gogusev J, Chretein Y, Iris L. Expression of the human nephron differentiation molecules in renal cell carcinomas. *Am J Pathol*. 1990; 137 (4): 895-905.
29. Eck W, Nicholson AI, Zentgraf H, Semmler W, Bartling S. Anti-CD4-targeted gold nanoparticles induce specific contrast enhancement of peripheral lymph nodes in X-ray computed tomography of live mice. *Nano Lett*. 2010; 10 (7): 2318-2322.
30. Kristiansen G, Denkert C, Schluns K, Dahl E, Pilarsky C, Hauptmann S. CD24 is expressed in ovarian cancer and is a new independent prognostic marker of patient survival. *Am J Pathol*. 2002; 161 (4): 1215-1221.
31. Liu W, Vadgama JV. Identification and characterization of amino acid starvation-induced CD24 gene in MCF-7 human breast cancer cells. *Int J Oncol*. 2000; 16(5): 1049-1054.
32. Welsh JB, Zarrinkar PP, Sapinoso LM, Kern SG, Behling CA, Monk BJ, Lockhart DJ, Burger RA, Hampton GM. Analysis of gene expression profiles in normal and neoplastic ovarian tissue samples identifies candidate molecular markers of epithelial ovarian cancer. *Proc Natl Acad Sci. U. S. A* 2001; 98(3): 1176-1181.
33. Kappelmayer J, Nagy BJ. The Interaction of Selectins and PSGL-1 as a Key Component in Thrombus Formation and Cancer Progression. *Biomed Res Int*. 2017; 6138145.
34. Wang L, Liu Q, Hu Z, Zhang Y, Wu C, Yang M, Wang P. A novel electrochemical biosensor based on dynamic polymerase-extending hybridization for E. coli O157:H7 DNA detection. *Talanta*. 2009; 78(3): 647-652.
35. Cai QY, Kim SH, Choi KS, Kim SY, Byun SJ, Kim KW, Park SH, Juhng SK, Yoon KH. Colloidal gold nanoparticles as a blood-pool contrast agent for X-ray computed tomography in mice. *Invest Radiol*. 2007; 42(12): 797-806.
36. Lusic H, Grinstaff MW. X-ray-computed tomography contrast agents. *Chem Rev*. 2013; 113(3): 1641-1666.
37. Adumeau L, Genevois C, Roudier L, Schatz C, Couillaud F, Mornet S. Impact of surface grafting density of PEG macromolecules on dually fluorescent silica nanoparticles used for the in vivo imaging of subcutaneous tumors, *Biochim Biophys Acta*. 1861(6) (2017): 1587-1596.

38. Macharia DK, Tian Q, Chen L, Sun Y, Yu N, He C, Wang H, Chen Z. PEGylated (NH<sub>4</sub>)<sub>2</sub>WO<sub>3</sub> nanorods as efficient and stable multifunctional nanoagents for simultaneous CT imaging and photothermal therapy of tumor, *J Photochem Photobiol B.* 174(2017): 10-17.
39. Vlerken Van LE, Vyas TK, Amiji MM. Poly(ethylene glycol)-modified nanocarriers for tumor-targeted and intracellular delivery, *Pharm Res.* 24(8) (2007): 1405-1414.